Available online at www.sciencedirect.com
ScienceDirect
Biomaterials 28 (2007) 2582–2589
Biomaterials
www.elsevier.com/locate/biomaterials

Bone formation at the surface of low modulus Ti–7.5Mo implants in rabbit femur

Dan-Jae Lin[a,b], Cheng-Chung Chuang[a], Jiin-Huey Chern Lin[a], Jing-Wei Lee[c], Chien-Ping Ju[a], Hsiang-Shu Yin[b,*]

[a]*Department of Materials Science and Engineering, National Cheng-Kung University, Tainan, 701, Taiwan, ROC*
[b]*Department of Anatomy and Cell Biology, College of Medicine, National Taiwan University, Taipei 100, Taiwan, ROC*
[c]*Division of Plastic Surgery, Department of Surgery, National Cheng-Kung University Hospital, Tainan 701, Taiwan, ROC*

Received 27 December 2006; accepted 6 February 2007
Available online 15 February 2007

Abstract

The biocompatibility of the Ti–7.5Mo alloy was examined, because the alloy has a high-strength/modulus ratio and thus is a potential candidate for orthopedic applications. Cell viability assay using 3T3 cells revealed that the Ti–7.5Mo did not induce apparent cell death, when the cells were grown on disks made of the alloy or incubated with the alloy-conditioned medium at 37 or 72 °C for 24–72 h. The Ti–6Al–4V alloy was used as a control and did not cause apparent cell death either. Moreover, pins of 6 mm long and 2 mm in diameter of Ti–7.5Mo and Ti–6Al–4V were implanted into the left and right rabbit femurs, respectively, for 6, 12 and 26 weeks. New bone tissue grew to surround the pins, which spanned cortical and marrow regions, as shown by toluidine blue-stained bone sections of the three time points. Strikingly, the amount of new bone encircling the Ti–7.5Mo implant was approximate two-folds of that at Ti–6Al–4V by 26 weeks post-implantation. This facilitation of bone formation could be associated with the unique properties, such as a low modulus and the composition of Mo, of the Ti–7.5Mo.

Keywords: Cell viability; Implantation to femur; Bone growth; Bone marrow; Bioabsorption

1. Introduction

Titanium (Ti) and its alloys have been utilized in medical practice, for they have high-strength/density ratios, excellent corrosion resistance to biological environments, and strong adhesion to bone tissue [1]. Nevertheless, the clinically used Ti–6Al–4V has an elastic modulus of 110 GPa, which is lower than 210 GPa of Co–Cr–Mo and 200 GPa of stainless steel, but still higher than 25 GPa of natural bone [2]. A significant difference in stiffness between implants and bone tissue can lead to stress shielding effect, and thereby may cause osteoporosis or poor osseointegration, while an implant with a low elastic modulus shares loads with the bone to facilitate bone growth [3–5].

Ti alloys containing beta-stabilizer elements, such as Mo, Nb or Ta, displayed low elastic modulus and superior corrosion resistance [6,7]. Furthermore, Mo ions are thought to be less toxic than Al and V, as shown by cell culture studies [8,9]. A number of Ti–Mo alloys have been applied to clinical surgery, such as Ti–12Mo–6Zr–2Fe [10] (TMZF®, Howmedica Osteonics Corp., USA) and Ti–15Mo–5Zr–3Al [11] (Kobe Steel Ltd., Japan). However, these alloys still contain Fe and Al, which are among the potentially toxic metal ions.

A Ti–7.5 wt% Mo alloy without Fe or Al has been developed by Chern Lin et al. [12] and possesses an α'' phase structure as well as a low modulus of 65 GPa. The ratio of bending strength to modulus (MPa/GPa) of Ti–7.5Mo is 25.4, substantially higher than that of commercial pure Ti (9.6) and Ti–6Al–4V (17.4) alloy [13], and thus implies excellent mechanical properties for clinical application.

*Corresponding author. Fax: +886 2 23959284.
E-mail address: hsyin@ha.mc.ntu.edu.tw (H.-S. Yin).

0142-9612/$ - see front matter © 2007 Elsevier Ltd. All rights reserved.
doi:10.1016/j.biomaterials.2007.02.005

A number of studies have disclosed that the chemical composition of titanium alloy is associated with the extent of cell differentiation. It has been found that MG63 osteoblast-like or rat bone marrow cells showed higher levels of differentiation, when they were grown in vitro on commercial pure Ti (cpTi) than on Ti–6Al–4V [14,15]. In addition, the Ti–29Nb–13Ta–4.6Zr was more biocompatible than cp Ti and Ti–6Al–4V, as revealed by greater viability of cultured L929 fibroblasts and MG63 cells in cell–alloy contact studies [16,17]. Nonetheless, the effect of Ti–7.5Mo demands investigation on viability of cells in culture.

A previous study demonstrated that the soft tissue reaction layers were not significantly different between Ti–15Mo–5Zr–3Al and cp Ti plates at 12 weeks after implantation, which were mounted on the rabbit tibia underneath an extensor muscle by using two screws, 1.5 mm in diameter [18]. However, changes in bone tissue are unclear around the implant. Furthermore, at 2 weeks following the implantation of a Ti-made hollow device into the rabbit tibia, bony trabeculae were formed within the isolated channel, whereas this newly formed bone developed into bone marrow tissue at 4–7 weeks post-implantation [19]. Hence, a constant contact force or mechanical movements and/or other parameters may be required to maintain a persistent growth of bone.

A number of studies have suggested that various surface conditions of Ti implants may affect the levels of bone formation on the implants. It has been shown that a rougher implant surface could induce better integration between bone and implant [20–22]. However, the relationship awaits clarification between quantitative responses of bone tissue and chemical composition/mechanical properties of Ti alloys.

Thus, the goal of the present study was to examine the level of bio-integration of the Ti–7.5Mo alloy by using Ti–6Al–4V as the control. A cylindrical device made of the alloy was implanted into the femur of the rabbit; the level of bone formation around the implant was monitored by histological methods at various post-implantation time points. Furthermore, the viability of cultured fibroblast cells was examined after they were plated on the alloy surface or incubated with the alloy-conditioned medium.

2. Materials and methods

2.1. Alloy preparation

The Ti–7.5 wt% Mo alloy was made from the titanium rod, 99.2% in purity, and Mo wire, 99.5% in purity, by using a commercial arc-melting and vacuum–pressure type casting system (Castmatic, Iwatani Corp., Japan). The melting chamber was first purged with argon, and an argon pressure of 1.5 kgf/cm^2 was maintained during the melting process. Appropriate amounts of metals were melted in a U-shaped copper hearth with a tungsten electrode. The Ti–Mo ingots were re-melted three times to improve chemical homogeneity. Ti–6Al–4V ingots were cut from a commercial Ti–6Al–4V (ELI) rod and melted. The difference in pressure between the melting and casting chambers allowed the molten alloys to instantly fall into a graphite mold at room temperature. The Ti alloys were fabricated and tested at the Department of Materials Science and Engineering of National Cheng Kung University.

Disks of the alloys, 1 mm in thickness and 6 mm in diameter, were prepared for cell culture experiments, and pins, 6 mm in length and 2 mm in diameter for in vivo experiments. The surface of the alloy specimens was sandblasted with 250 μm alumina particles (Korox® 250 BEGO, Bremen, Germany) and passivated with HF/HNO_3 acid. The surface of the specimens was observed under a scanning electron microscope (HITACHI S4200 Field Emission SEM) and the degree of roughness was measured by using a surface roughness meter (Surfcorder, SE-40D, Kosaka Laboratory Ltd.) (Figs. 1a and b). All specimens were cleaned with acetone for 20 min and distilled water 20 min, followed by sterilization in an autoclave at 121 °C for 30 min.

2.2. Cultured cells and the alloys

The effect of the alloys on the cell viability was examined by using cultured 3T3 fibroblasts (Balb/3T3 clone A31 from the embryo of BALB/C mouse). For contact test, Ti alloy disks were made from a casting rod and machined to a disk shape. Al_2O_3 powder was compressed into a mold and sintered at 1400 °C to form a dense disk. For the direct contact experiment, individual disks of Ti–7.5Mo or Ti–6Al–4V ($n = 5$) were placed in individual wells of 96-well plastic culture dishes (polystyrene, Nunclon™Δ). Sintered Al_2O_3 disks, presumably non-toxic to cells, and polyvinyl chloride (PVC) disks, toxic to cells, were prepared with the same size as that of Ti–7.5Mo ($n = 6$), and used as control groups for the direct contact experiment. The cells were plated at 5×10^3 cells/well in 100 μl DMEM (Dulbecco's Modified Eagle's Medium, Gibco) containing 10% fetal bovine serum and 1% antibiotic–antimycotic, and incubated in 5% CO_2 air at 37 °C for 24 h. Cells plated on six of 96 wells without alloys were used as a blank control group. After the incubation, the cells were washed with PBS and fed with 100 μl fresh culture medium/well. 10 μl of water-soluble tetrazolium salt (WST in WST Assay kit, Takara, Japan) was added to each well and the cells were incubated for 1 h.

The WST assay is based on that the tetrazolium salts are cleaved to become formazan by succinate dehydrogenase located at the mitochondrium. A reduction in the number of viable cells (with constant cell metabolism) or in the metabolic activity (within the same number of cells) results in decreased overall activity of mitochondrial dehydrogenases in the sample. This decline in enzyme activity leads to a decreased amount of formazan dye, correlating directly with a reduced viability of metabolically active cells in the culture. The levels of formazan production were measured in the cells by using an ELISA reader at an absorbance of 450 nm.

In order to examine whether a possible release of ions and/or other substances from the alloys affects the cultured cells, the conditioned medium was prepared in a separate experiment. The conditioned medium was obtained by placing the alloy disk (3 cm^2/ml) or control materials (Al_2O_3 powder 0.2 g/ml, non-toxic to cells, or 0.3% phenol, toxic to cells) in the culture medium within a 45 ml polyethylene centrifuge tube at 37 ± 2 °C for 72 h or 70 ± 2 °C for 24 h. The 70 °C incubation was used to investigate the effects of high temperature on the possible release of ions/substances from the alloys. The 3T3 cells were plated on 96-well culture dishes and incubated with the conditioned medium for 24 or 48 h. Afterwards, the viability of cells was determined using the WST assay. Data are presented as means ± SD and were compared among various experimental groups with one-way ANOVA and Tukey's post hoc comparison (Origin 7.0, USA). A p value of less than 0.05 is considered statistically significant.

2.3. Implantation in rabbit femurs

Adult male New Zealand rabbits of 2.5–3 kg in weight were kept at 25 °C with free access to food and water for 2 weeks before surgery ($n = 30$). The rabbits were anesthetized by an intramuscular injection of ketamine HCl/xylazine (Rompun®), 40/10 mg/kg, and then subjected to continuous intravenous injection of normal saline solution. The knee joint

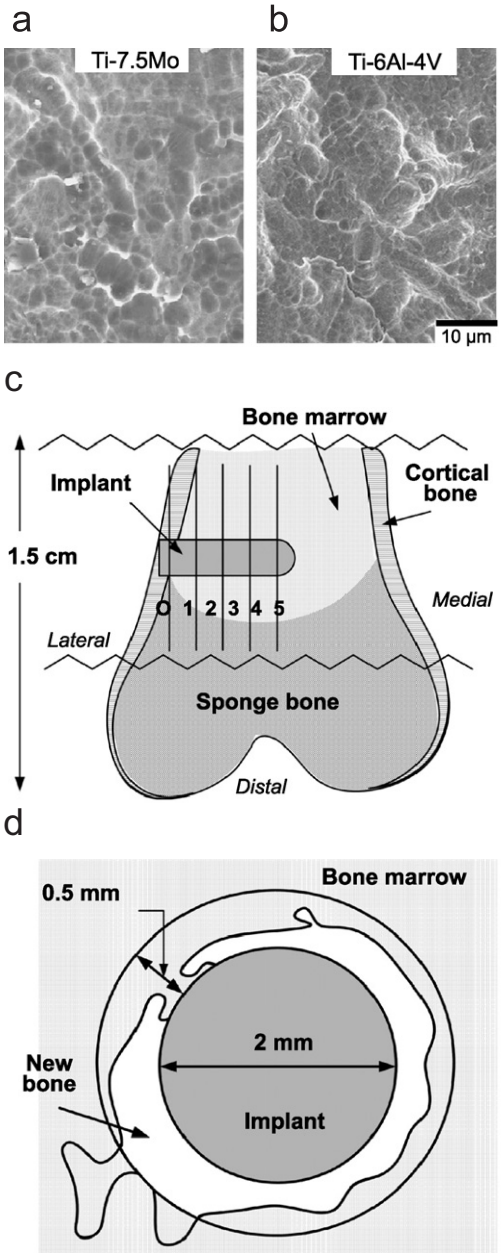

Fig. 1. The surface morphology of the implant (a, b) and implantation scheme (c, d). Scanning electron micrographs of the two implant alloys show similar surface morphology after sandblasting and acid etching, as described in the materials and methods (a, b). (c) Schematic drawing of the implant within the femur. The bone segment including implant, about 1 cm long (indicated by the two serrate lines), is removed at 6, 12 and 26 weeks post-implantation, fixed with formalin, and embedded in methylmethacrylate. Six sagittal sections, O and 1–5, are cut by a diamond saw. Diagram (d) shows a representative sagittal section of the implant-containing bone tissue, and illustrates the measurement of new bone formation. On each section after polishing and staining with toluidine blue, the total area of new bone was measured within the concentric circle of the implant, 3 mm in diameter.

region was scrubbed with tincture of iodine and 70% ethanol; the animal was then given local anesthetics of atropine, 0.001 mg/kg, by subcutaneous injection. A hand drill with a screw rod of 2 mm in diameter and 7 mm long was used to drill a hole through the cortical bone, trabeculae and bone marrow, which was located at the lateral side of femur and 10 mm proximal to its distal end. Individual Ti–7.5Mo and Ti–6Al–4V alloy pins were pressed into the pre-drilled holes of the left and right femurs, respectively (Fig. 1c).

After survival periods of 6, 12, and 26 weeks, the rabbits were sacrificed by using intravenous injection of 15% potassium chloride, 1.5 ml/kg, in conjunction with the ketamine anesthesia. The distal piece of each femur, spanning 10 mm long containing the Ti alloy pin, was fixed with 10% neutral buffered formalin pH 7 at 4 °C for 3 days and dehydrated with a series of graded ethanols (Fig. 1b). The samples were then embedded in methylmethacrylate (MMA) [23] and sliced into six saggital sections of 250 μm thickness, from lateral to medial, section O, and 1–5, by using a Buehler low speed diamond saw (Fig. 1c). The animal experiment was performed at the animal center of Medical College of NCKU, in accordance with the guidelines of the animal research committee of NCKU.

The most laterally located Section O was gently polished, sputtered with gold and observed under a scanning electron microscope (Philips XL40 FE-SEM). Sections 1–5 were polished to a final thickness of about 60 μm, and glued to glass slides with Permount (Fisher Scientific, USA). The samples were stained with toluidine blue and investigated by using a Leica microscope (Leitz Labrorlux 12 Pols, Leica Co., Germany) with a Nikon digital camera (Nikon coolpix 995, Japan). The areas of new bone tissue enclosing the implant were measured within a circle, 2.5 mm in diameter, concentric with the implant pin on each section using a computer program (Image Pro) (Fig. 1d). Levels of bone growth were analyzed and compared among 1–5 sections in relation to post-implantation times and between the alloy types using two-way ANOVA followed by Tukey's post hoc comparison.

2.4. Immunocytochemistry

The bone tissue containing the implant was fixed with 10% formalin in 0.1 M phosphate buffer, pH 7.4, for 48 h at 4 °C and decalcified in 7% EDTA in PBS, pH 7.4, for 14 days. The implant in the sample was removed and the sample was dehydrated by using a graded series of ethanols. After embedding in paraffin, 7-μm-thick sections of the sample were obtained. The immunostaining was carried out according to a previous protocol [24]. Briefly, the paraffin sections were deparaffined, and blocked with 1.25% normal serum before incubated with the anti-vitamin D or anti-vimentum antibodies (Sigma, St. Louis, USA), diluted 1:500 or 1:100 in PBS, for 16 h at 4 °C. The anti-vitamin D antibody labels the osteoblasts/osteocytes, and the anti-vimentum antibody the fibroblasts/mesenchymal cells. Thereafter, the samples were incubated with a biotinylated secondary antibody, followed by visualization of immunoreaction products by the ABC-peroxidase method (Vector) using 3,3′-diaminobenzidine tetrahydrochloride (DAB) as the chromagen.

3. Results

3.1. Viability of cultured cells

As detected by the WST-1 assay, the viability levels of 3T3 cells showed significant differences after they were grown on different substrates, Ti–7.5Mo, Ti–6Al–4V, Al_2O_3, PVC and blank (culture dish), for 24 h at 37 °C ($F(5, 20) = 10.21$, $p < 0.001$). The viability of cells on Ti–7.5Mo was similar to that on Ti–6Al–4V, whereas higher than Al_2O_3; cells on these three groups together with the blank had higher viability than the cells on PVC ($p < 0.05$–0.001) (Fig. 2a).

When cells were incubated for 24 or 48 h with the conditioned medium, prepared from incubation with the Ti–7.5Mo alloy, Ti–6Al–4V alloy, Al_2O_3 or blank group at 37 °C for 72 h or at 70 °C for 24 h, they showed higher viability than that incubated with 0.3% phenol (37 °C/72 h,

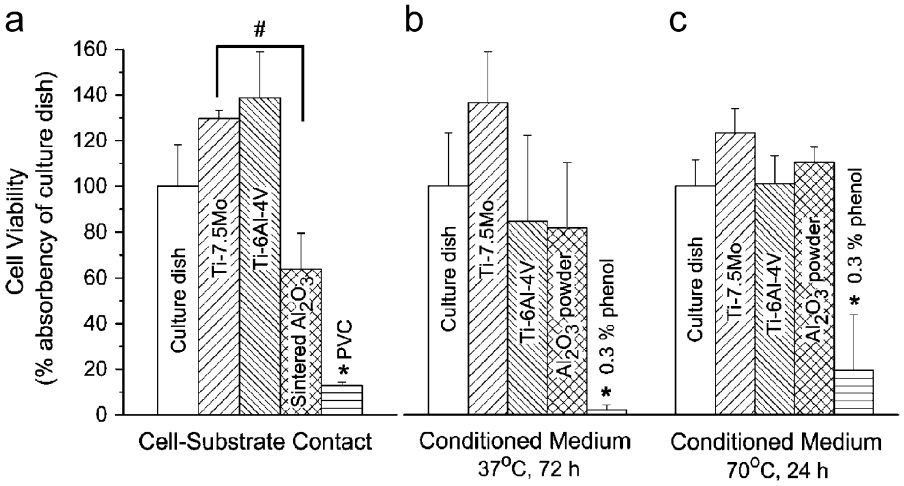

Fig. 2. Ti–7.5Mo and Ti–6Al–4V alloys do not induce apparent death of cultured cells. For the cell-substrate direct contact experiment, the viability of 3T3 cells was examined by using a WST assay kit, after they were plated on Ti7.5Mo, Ti–6Al–4V, sintered Al_2O_3, culture plate (blank control), and PVC for 24 h at 37 °C (a). For cell–alloy extract contact experiment, 3T3 cells were incubated with conditioned medium for 24 h, which was obtained from incubation with Ti–7.5Mo, Ti–6Al–4V, Al_2O_3 or blank or with 0.3% phenol at 37 °C for 72 h or 70 °C for 24 h. *: $p<0.05$, compared with either of the other conditions within one group; #: $p<0.05$, comparison between Ti–7.5Mo and sintered Al_2O_3.

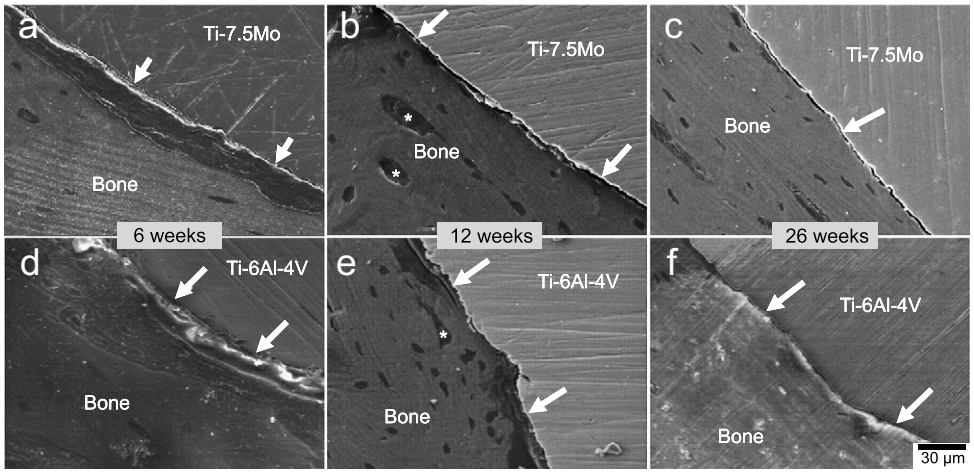

Fig. 3. Scanning electron micrographs of the section O show the interface between new bone and Ti–7.5Mo or Ti–6Al–4V implant at 6 weeks (a, d), 12 weeks (b, e), and 26 weeks post-implantation (c, f). The implant is closely opposed with the bone tissue (arrows). At 6 weeks, a relatively darker zone of presumable soft-bone is seen adjacent to the implant for both alloys (a, d). At 12 and 26 weeks, this zone is apparently replaced by hard bone, containing osteons (asterisks) and lacunae (b, e, c, f).

$F(4, 19) = 13.03$ for 24 h, and $F(4, 19) = 11.66$ for 48 h, $p<0.001$; 70 °C/24 h, $F(4, 18) = 17.28$ for 24 h, and $F(4, 19) = 26.00$ for 48 h, $p<0.001$) (Fig. 2b).

3.2. Histological observations

SEM analysis showed that the surfaces of the Ti–7.5Mo and Ti–6Al–4V pins had similar morphology after the sandblast-etching treatment (Figs. 1a and b). The surface roughness of the Ti–7.5Mo, 1.48 ± 0.08 μm, was similar to 1.51 ± 0.12 μm of Ti–6Al–4V ($n=6$). The extent of integration was examined between the Ti–7.5Mo implant and bone tissue on Section O, which included the cortical bone. At 6 weeks, a zone of soft tissue or pre-bone tissue was seen between the implant and cortical bone for both alloys (Figs. 3a and d). At 12 weeks, the bone tissue presumably replaced the soft tissue and contained lacunae that indicated the presence of osteocytes (Figs. 3b and e). By 26 weeks, the lamellar bone was seen in close proximity to the implant (Figs. 3c and f).

In general, newly formed bone tissue was seen surrounding the implants of the Ti–6Al–4V and Ti–7.5Mo alloys at levels of Section O and 1–5 at 6–26 weeks post-implantation, in the absence of macrophages, as revealed by toluidine blue-stained bone sections. At 6 weeks post-implantation, on Section 1, the surface of the implant was encircled by new bone tissue; adjacent to the implant there were bone trabeculae and the spaces were filled with bone

marrow, containing many fat cells and blood cells (Fig. 4c). After 26 weeks, the new compact bone had become significantly thicker, compared with that at 6 weeks (Fig. 4d). The presence of osteoblasts or osteocytes was verified in the bone tissue by immunostaining with a specific antibody to vitamin-D receptor (Fig. 4e). The osteoblasts/osteocytes were seen scattered in the newly formed bone tissue adjacent to the implant. The amount of the new bone gradually decreased from Sections 1 to 5 at each of the post-implantation times (Fig. 5).

3.3. Ti–7.5Mo alloy

At 6 weeks post-implantation, the mean areas of new bone encircling the implant were $1.66 \pm 0.24\,mm^2$ on Section 1, $1.34 \pm 0.33\,mm^2$ Section 2, $1.01 \pm 0.21\,mm^2$ Section 3, $0.58 \pm 0.21\,mm^2$ Section 4, and $0.18 \pm 0.15\,mm^2$ Section 5 (Fig. 6a) within the 0.5 mm wide circle band enclosing the implant. Significant differences were found among these values ($F(4, 20) = 25.08$, $p < 0.001$). The area of Section 1 was similar to that of Section 2, while larger than that of Section 3 ($p < 0.05$), 4 ($p < 0.001$) and 5 ($p < 0.001$); the Section 2 had larger new bone area than Section 4 ($p < 0.01$) and 5 ($p < 0.001$), and Section 3 larger than 5 ($p < 0.01$).

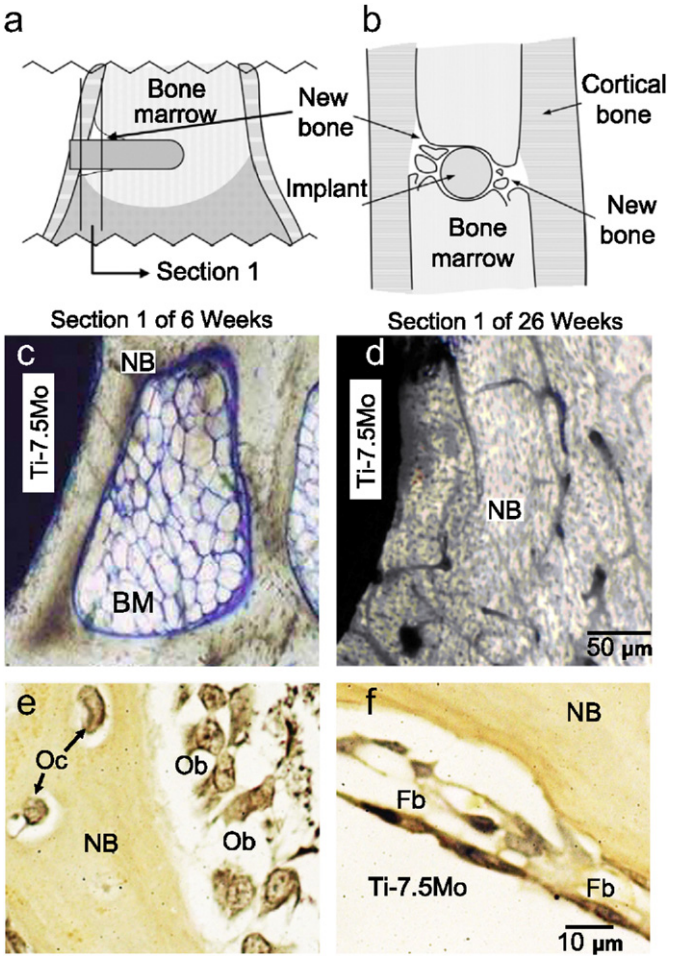

Fig. 4. Micrographs illustrate the time course of new bone formation in Section 1 and immunocytochemical evidence of osteoblasts in the new bone. (a) Diagram of a coronal view of the implantation site indicates the new bone abutting the implant. (b) Illustration of Section 1 shows relative positions of implant, new bone and bone marrow. (c, d) Micrographs show the new bone formed around Ti–7.5Mo alloy on Section 1 at 6 and 26 weeks post-implantation. New bone (NB) and interspersed bone marrow tissue (BM) enclose the implant. The osteoblasts (Ob) and osteocytes (Oc) are verified by immunocytochemistry using an anti-vitamin D receptor antibody (e), and the fibroblasts (Fb) an anti-vimentin antibody (f).

By 12 weeks, the area means were also different among Sections 1–5 ($F(4, 20) = 34.69$; $p < 0.001$). The area of Section 1, $3.01 \pm 0.43\,mm^2$, was larger than $1.97 \pm 0.46\,mm^2$ of Section 2 ($p < 0.01$), $1.27 \pm 0.22\,mm^2$ of Section 3 ($p < 0.001$), $0.70 \pm 0.30\,mm^2$ of Section 4 ($p < 0.001$), and $0.67 \pm 0.16\,mm^2$ of Section 5 ($p < 0.001$). The area of Section 2, $1.99 \pm 0.92\,mm^2$ was larger than that of Sections 4 and 5 ($p < 0.001$). At 26 weeks, the bone area of Section 1, $3.24 \pm 0.51\,mm^2$, was larger than Section 3 ($1.54 \pm 0.86\,mm^2$) ($p < 0.05$), Section 4 ($1.35 \pm 0.51\,mm^2$) ($p < 0.001$), and Section 5 ($1.42 \pm 0.50\,mm^2$) ($p < 0.05$) ($F(4, 20) = 5.24$; $p < 0.01$). The values were similar among Sections 2–5.

On the Section 1 of 6 weeks, the area of new bone was smaller than that of 12 and 26 weeks, whereas the latter two had analogous values of new bone ($F(2, 12) = 17.40$, $p < 0.001$). The new bone areas of Sections 2–4 were similar among the three time points. For Section 5, the values of 6 and 12 weeks were similar, but both were smaller than that of 26 weeks ($F(2, 12) = 15.49$, $p < 0.05$).

3.4. Ti–6Al–4V alloy

By 6 weeks after implantation, differences in areas of new bone were seen surrounding the implant among Sections 1–5 ($F(4, 20) = 37.48$; $p < 0.001$) (Fig. 6b). Bone areas of Section 1 ($1.57 \pm 0.24\,mm^2$) and Section 2 ($1.45 \pm 0.22\,mm^2$) were larger than that of Section 3 ($1.02 \pm 0.15\,mm^2$) ($p < 0.001$, $p < 0.05$), Section 4 ($0.63 \pm 0.15\,mm^2$) ($p < 0.001$) and 5 ($0.2 \pm 0.15\,mm^2$) ($p < 0.001$), whereas both areas of Sections 3 and 4 were larger than that of Section 5 ($p < 0.001$, $p < 0.05$).

At 12 weeks post-implantation, there were differences in new bone areas among the five sections ($F(4, 20) = 18.81$, $p < 0.001$). The bone area of Section 1 ($2.78 \pm 0.42\,mm^2$) and 2 ($2.3 \pm 0.35\,mm^2$) were larger than Section 3 ($0.69 \pm 0.34\,mm^2$) ($p < 0.001$, $p < 0.01$), 4, $0.45 \pm 0.19\,mm^2$ ($p < 0.001$, $p < 0.01$) and 5, $1.08 \pm 0.63\,mm^2$ ($p < 0.05$). No significant differences were found among the areas of Sections 3–5. By 26 weeks, there were significant differences among the values of these five sections ($F(5, 20) = 100.87$; $p < 0.001$). The bone area of Section 1 ($3.27 \pm 0.30\,mm^2$) was larger than that of Section 2–5 ($p < 0.001$). Similar values were seen among the areas of Section 2 (0.57 ± 0.19), 3 (0.24 ± 0.15), 4 (0.12 ± 0.07), and 5 (0.12 ± 0.06).

The new bone area of Section 1 at 6 weeks was smaller than that of 12 and 26 weeks ($F(2, 12) = 30.17$; $p < 0.05$); similar areas were observed at 12 and 26 weeks. In

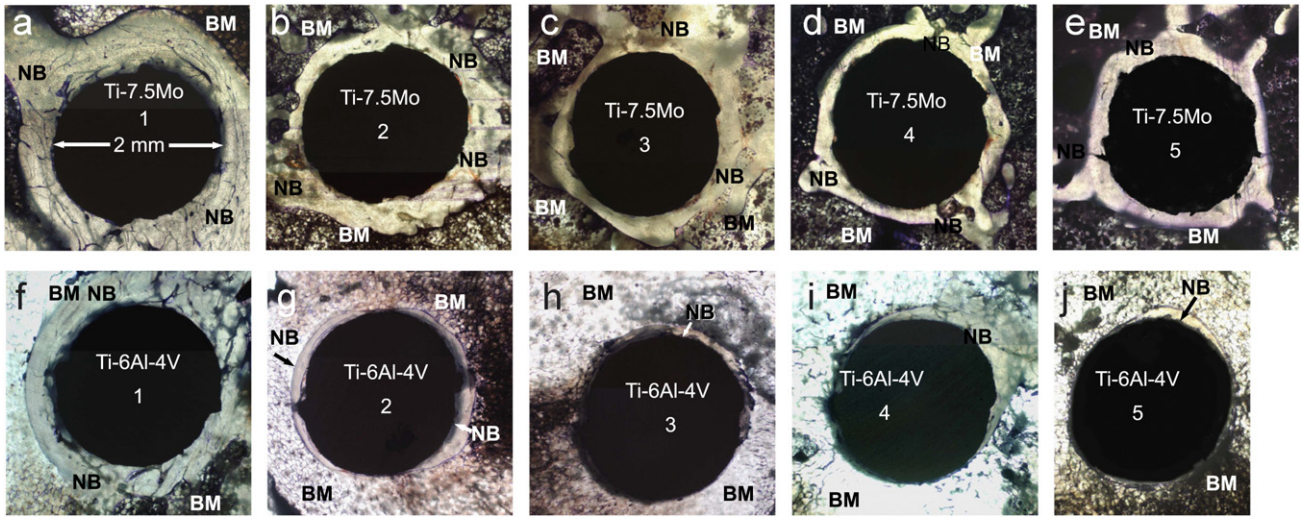

Fig. 5. An overview of new bone formation on major parts of the implant within the femur at 26 weeks post-implantation. Micrographs show serial sagittal Sections 1–5 of the bone including Ti–7.5Mo (a–e) or Ti–6Al–4V implant (f–j). The sections were stained with toluidine blue. New bone (NB) encircles almost completely the Ti–7.5Mo implant on all five sections and Sections 1 and 2 of the Ti–6Al–4, whereas partially the Sections 3–5 of Ti–6Al–4V. Bone marrow (BM) is in close proximity to parts of the brim of the Ti–6Al–4V implant at Sections 3–5. The respective bone areas of Sections 2–5 of Ti–7.5Mo group are larger than that of corresponding sections of Ti–6Al–4V.

Section 2, the bone area of 12 weeks was larger than that of 6 weeks; the area of 6 weeks was larger than 26 weeks ($F(2, 12) = 41.43$; $p < 0.01$). Similar areas were seen at 6 and 12 weeks of Section 3, and both were larger than 26 weeks ($F(2, 12) = 13.55$; $p < 0.01$). The three section 4s of 6, 12, and 26 weeks had analogous new bone areas. The area of Section 5 at 12 weeks was larger than that of 6 and 26 weeks ($F(2, 12) = 8.556$; $p < 0.05$); the values of the latter two time points were similar.

Comparison of new bone formation between the Ti–7.5Mo and Ti–6Al–4V alloys showed that at 6 and 12 weeks post-implantation, there were no significant differences in new bone areas between comparable sections of Ti–7.5Mo and Ti–6Al–4V. Strikingly, by 26 weeks, the areas of sections of Ti–Mo revealed significant differences from that of Ti–6Al–4V ($F(4, 40) = 2.67$, $p < 0.05$). The bone areas at Ti–7.5Mo of Sections 2–5 were larger than that of comparable sections of the Ti–6Al–4V ($p < 0.05$). The sum of the bone areas of all 5 sections at the Ti–7.5Mo implant was approximate 221% of that of Ti–6Al–4V.

4. Discussion

The present study revealed that at 26 weeks after implantation in the rabbit femur, a greater amount of new bone was formed at the Ti–7.5Mo alloy than the Ti–6Al–4V alloy. Possible absorption of new bone tissue was proposed at the Ti–6Al–4V implant, whereas was absent around the Ti–7.5Mo implant. The facilitation of bone formation at Ti–7.5Mo may be associated with the low modulus and other characteristics of the alloy.

Among the five serial bone Sections 1–5 that included sections of the implant, the laterally located Section 1, being closest to the cortical and sponge bone, contains the largest new bone area around the implant of Ti–7.5Mo or Ti–6Al–4V at 12 and 26 weeks following implantation. This is probably owing to that Section 1 was nearest to the endosteum of the cortical bone, from which new bone tissue at the implant originated. An earlier work using electron microscopy supported that the osteoblasts of endosteum of cortical or trabecular bone could migrate to the titanium implant/bone marrow interface and undergo intramembranous bone formation [25].

The new bone in Section 2 of Ti–7.5Mo group, similar to that of Section 1, may have also originated from the endosteum, and remained constant in amount throughout 26 weeks. By contrast, although at 6 and 12 weeks, the Section 2 of Ti–6Al–4V contained similar levels of new bone to that of Ti–Mo, at 26 weeks the bone area of Ti–6Al–4V Section 2 became less than that of 6 and 12 weeks, implying a retraction or absorption of the new bone tissue at Ti–6Al–4V. Resembling Section 2 of Ti–7.5Mo, Section 3 of Ti–7.5Mo had similar new bone areas at the three time points, whereas the bone area of Section 3 of Ti–6Al–4V was smaller at 26 weeks than 12 weeks, and again implicates bone retraction.

A previous study similarly reported the absorption of newly grown bone tissue on an implant in a marrow cavity [19]. The new bone trabeculae were first formed and later developed into bone marrow tissue in the isolated channel of a hollow Ti device in medullary cavity of rabbit tibia. In our study, unlike the inconsistent bone formation at Ti–6Al–4V, the Ti–7.5Mo alloy induced persistent bone growth without absorption with post-surgery time, indicating its unique biocompatible characteristics.

On Section 5, the level of new bone at 6 weeks was the least among five sections of both alloys. For Ti–6Al–4V, the new bone of Section 5 was larger at 12 weeks than

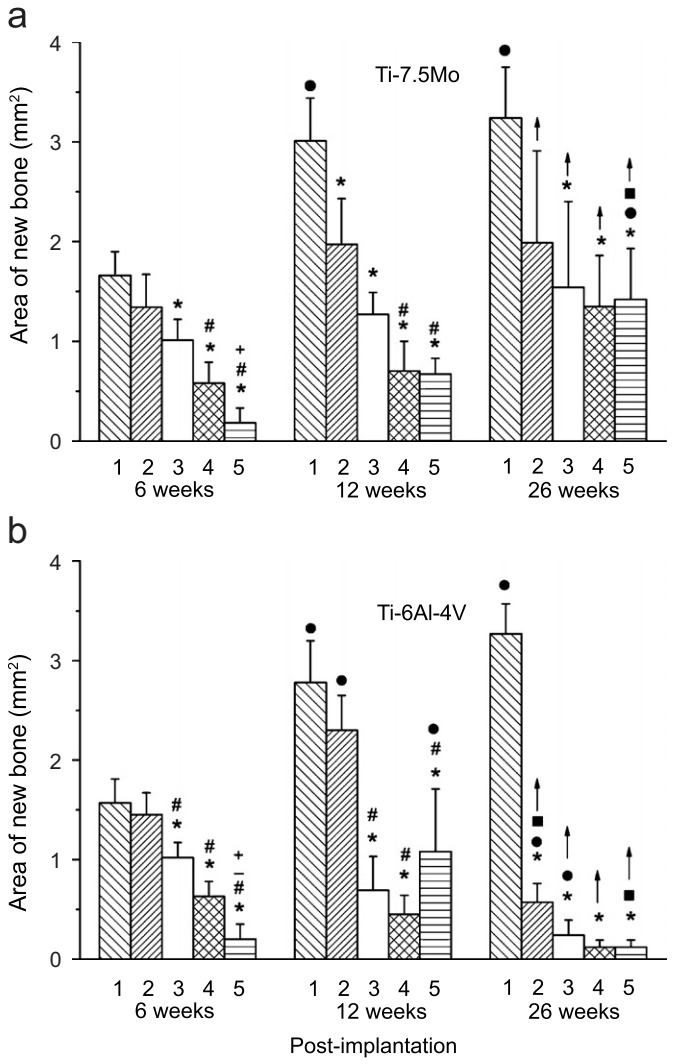

Fig. 6. Time course of quantitative new bone growth surrounding the entire implant at 6 weeks, 12 weeks, and 26 weeks post-implantation. Serial bone sections including the implant were stained with toluidine blue. Areas of new bone were measured on the sections ($n = 5$) as described in Materials and Methods (Fig. 1b); data points are means±SD. *: Significantly different from Section 1; #: significantly different from Section 2; +: significantly different from Section 3; —: significantly different from Section 4; ●: significantly different from 6 weeks; ■: significantly different from 12 weeks; ↑: significantly different between Ti–7.5Mo and Ti–6Al–4V, $p<0.05$.

6 weeks and 26 weeks. This likewise suggests a growth at 12 weeks and retraction at 26 weeks for Ti–6Al–4V. In contrast, the new bone on Section 5 of Ti–Mo at 26 weeks was strikingly larger than that of 6 weeks and 12 weeks, indicating a facilitated formation of new bone on the Ti–7.5Mo implant. Indeed at 26 weeks, the new bone area was greater on Sections 2–5 of Ti–7.5Mo than that of comparable sections of Ti–6Al–4V, and thereby denotes a higher level of bone growth on the Ti–7.5Mo alloy than Ti–6Al–4V.

The apparent enhancement of new bone formation on the Ti–7.5Mo implant may be associated with the characteristics of the alloy. The modulus of Ti–7.5Mo alloy, 65 Gpa, is lower than that of Ti–6Al–4V; the less stiff Ti–7.5Mo probably facilitates the bone formation. The lateral end of the implant was embedded in the cortical bone and the rest of it in the medullary cavity of femur. The lateral implant end may be anchored by the newly formed bone and micro-movements could occur in the relatively larger medial part of implant, which was in contact with the osteogenic cells of bone marrow. The micro-movement or strain of implant may be generated by the load from the cortical bone.

The micro-strain is thought to be necessary for the bone remodeling process [26]. Hence, it could be that the micro-strain of the Ti–7.5Mo implant participates in formation of the persistent new bone on the implant, which was formed by bone precursor cells of bone marrow. A lack of strain may occur at the implant-tissue interface for a stiffer material, such as Ti–6Al–4V. This may also account for, at least in part, the transformation of bone into bone marrow in the previous study using a hollow Ti chamber placed in bone marrow, where there was no load and lacked micro-strain [19].

In our work, no apparent differences were found in the surface morphology and alloy/bone interface between the Ti–7.5Mo and Ti–6Al–4V. Although researches have suggested that surface characteristics of implant are important to the success of bone formation, it seems that different levels of bone growth in our study do not come from the surface features of the alloys [20,21]. However, further study is needed to investigate the detailed interaction between the alloy and bone tissue using transmission electron microscopy.

It has been proposed that ions released by implant are associated with the failure of clinical implantation of titanium alloy [27]. Ions released by Ti–6Al–4V alloy or Al^{+3} could inhibit the osteocalcin synthesis of bone marrow stromal cells or expression of osteocalcin and alkaline phosphatase of osteoblast-like cells in culture [28,29]. By contrast, the Mo ion has a smaller effect on proliferation, viability, type-I collagen gene expression, and cytokine release of osteoblasts than Al^{+3}, Ta^{+5}, Ni^{+2}, Fe^{+3}, and V^{+3} [8]. Our data from the cell culture experiment suggest that Ti–7.5Mo and Ti–6Al–4V alloys do not induce apparent cell death either in direct contact or conditioned-medium experiments. Despite that the incubation time was only 1–2 days, the results may indicate little effect of the surface composition and extracts of alloys on fibroblast viability. After long-term implantation in vivo, the Ti–7.5Mo alloy may be better incorporated into the bone tissue than Ti–6Al–4V. Nonetheless, the long-term effect of Ti–7.5Mo alloy requires to be explored on survival of cells in culture.

5. Conclusions

Our findings reveal that the Ti–7.5Mo implant induced a remarkably persistent growth of new bone enclosing itself in the rabbit femur, compared to the retraction of new

bone seen at the Ti–6Al–4V. Mechanisms underlying this enhanced bone formation probably involve the unique mechanical properties, and the generally good biocompatibility of the Ti–7.5Mo alloy. The results confirm that the Ti–7.5Mo alloy is an excellent candidate for clinical implantation applications.

Acknowledgments

This work was supported by a grant, NSC92-2321-B-002-001, provided by National Science Council of Taiwan.

References

[1] Kawahara H. Cellular responses to implant materials: biological, physical and chemical factors. Int Dent J 1983;33:350–75.
[2] Pilliar RM. Modern metal processing for improved load-bearing surgical implants. Biomaterials 1991;12:95–100.
[3] Uhthoff HK, Bardos DI, Liskova-Kiar M. The advantages of titanium alloy over stainless steel plates for the internal fixation of fractures. An experimental study in dogs. J Bone Joint Surg Br 1981;63B:427–84.
[4] Sumner DR, Turner TM, Igloria R, Urban RM, Galante JO. Functional adaptation and ingrowth of bone vary as a function of hip implant stiffness. J Biomech 1998;31:909–17.
[5] Gasser B. Design and engineering criteria for titanium devices. In: Brunette DM, Tengvall P, Textor M, Thomsen P, editors. Titanium in medicine. Berlin: Springer; 2001. p. 674.
[6] Long M, Rack HJ. Titanium alloys in total joint replacement—a materials science perspective. Biomaterials 1998;19:1621–39.
[7] Ankem S, Greene CA. Recent developments in microstructure/property relationships of beta titanium alloys. Mater Sci Eng 1999;A263:127–31.
[8] Hallab NJ, Vermes C, Messina C, Roebuck KA, Glant TT, Jacobs JJ. Concentration- and composition-dependent effects of metal ions on human MG-63 osteoblasts. J Biomed Mater Res 2002;60:420–33.
[9] Geurtsen W. Biocompatibility of dental casting alloys. Crit Rev Oral Biol Med 2002;13:71–84.
[10] Wang K. The use of titanium for medical applications in the USA. Mater Sci Eng 1996;A213:134–7.
[11] Okazaki Y, Ito Y. New Ti alloy without Al and V for medical implants. Adv Eng Mater 2000;2:S278.
[12] Chern Lin JH, Ju CP, Ho WF. Biocompatible low modulus titanium alloy for medical implant. US Patent No. 6409852, 2002.
[13] Ho WF, Ju CP, Lin JH. Structure and properties of cast binary Ti–Mo alloys. Biomaterials 1999;20:2115–22.
[14] Lincks J, Boyan BD, Blanchard CR, Lohmann CH, Liu Y, Cochran DL, et al. Response of MG63 osteoblast-like cells to titanium and titanium alloy is dependent on surface roughness and composition. Biomaterials 1998;19:2219–32.
[15] Rosa AL, Beloti MM. Rat bone marrow cell response to titanium and titanium alloy with different surface roughness. Clin Oral Impl Res 2003;14:43–8.
[16] Niinomi M. Fatigue performance and cyto-toxicity of low rigidity titanium alloy, Ti–29Nb–13Ta–4.6Zr. Biomaterials 2003;24:2673–83.
[17] Naganawa T, Ishihara Y, Iwata T, Koide M, Ohguchi M, Ohguchi Y, et al. In vitro biocompatibility of a new titanium–29niobium–13tantalum–4.6zirconium alloy with osteoblast-like MG63 cells. J Periodontol 2004;75:1701–7.
[18] Ungersböck A, Pohler O, Perren SM. Evaluation of the soft tissue interface at titanium implants with different surface treatments: experimental study on rabbits. Biomed Mater Eng 1994;4:317–25.
[19] Zhou H, Choong, Henderson S, Chou ST, Aspenberg P, Martin TJ, et al. Marrow development and its relationship to bone formation in vivo: a histological study using an implantable titanium device in rabbits. Bone 1995;17:407–15.
[20] Thomas KA, Cook SD. An evaluation of variables influencing implant fixation by direct bone apposition. J Biomed Mater Res 1985; 19:875–901.
[21] Buser D, Schenk RK, Steinemann S, Fiorellini JP, Fox CH, Stich H. Influence of surface characteristics on bone integration of titanium implants. A histomorphometric study in miniature pigs. J Biomed Mater Res 1991;25:889–902.
[22] Sul YT, Johansson CB, Roser K, Albrektsson T. Qualitative and quantitative observations of bone tissue reactions to anodized implants. Biomaterials 2002;23:1809–17.
[23] Erben RG. Embedding of bone samples in methylmethacrylate: an improved method suitable for bone histomorphometry, histochemistry, and immunohistochemistry. J Histochem Cytochem 1997;45:307–13.
[24] Yin HS, Chen CT, Lin TY. Age and region-dependent alterations in the GABAergic innervation in the brain of rat treated with amphetamine. Int J Neuropsycopharm 2004;7:35–48.
[25] Kawahara H, Nakakita S, Ito M, Niwa K, Kawahara D, Matsuda S. Electron microscopic investigation on the osteogenesis at titanium implant/bone marrow interface under masticatory loading. J Mater Sci Mater Med 2006;17:717–26.
[26] Wiskott HWA, Belser UC. Lack of integration of smooth titanium surfaces: a working hypothesis based on strains generated in the surrounding bone. Clin Oral Implants Res 1999;10:429–44.
[27] Jacobs JJ, Skipor AK, Black J, Urban RM, Galante JO. Release and excretion of metal in patients who have a total hip replacement component made of titanium-base alloy. J Bone Joint Surg 1991; 73A:1475–86.
[28] Thompson GJ, Puleo DA. Ti–6Al–4V ion solution inhibition of osteogenic cell phenotype as a function of differentiation time course in vitro. Biomaterials 1996;17:1949–54.
[29] Sun ZL, Wataha JC, Hanks CT. Effects of metal ions on osteoblast-like cell metabolism and differentiation. J Biomed Mater Res 1997; 34:29–37.